Hindawi
Wireless Communications and Mobile Computing
Volume 2022, Article ID 7099494, 13 pages
https://doi.org/10.1155/2022/7099494

Research Article

Marine Drifting Trajectory Prediction Based on LSTM-DNN Algorithm

Xianbin Li,[1] Kai Wang,[1] Min Tang,[1] Jiangyi Qin,[1] Peng Wu,[1] Tingting Yang,[2] and Haichao Zhang[1]

[1]*National Innovation Institute of Defense Technology, Academy of Military Science, No. 53, Dongdajie Road, Fengtai District, Beijing 100071, China*
[2]*Navigation College, Dalian Maritime University, Dalian 116026, China*

Correspondence should be addressed to Kai Wang; cxywangkai@163.com and Min Tang; mtangcn@163.com

Received 15 February 2022; Accepted 26 May 2022; Published 2 July 2022

Academic Editor: A.H. Alamoodi

In this paper, the long short-term memory with dense neural network (LSTM-DNN) is first introduced to calculate marine drifting trajectory. Based on the Internet of Things technology and the LSTM-DNN algorithm, the marine drifting trajectory model is established. In this model, the information such as wind field, temperature field, ocean current motion field, and target attributes are included, and the influences of the above information on the trajectory model are studied in detail. In order to verify the proposed model, the marine experiments are carried out in the end. The results show that the predicted trajectory data matches well with the experimental trajectory data. By introducing DNN into the algorithm, computational accuracy of drifting trajectory can be significantly improved compared with the conventional LSTM-based prediction model. A detailed comparison of the two algorithms has also been given in the paper. The proposed remote sensing of marine drifting trajectory model can provide a high accurate trajectory prediction and will lead an important guidance in the marine search and rescue work.

1. Introduction

In recent years, the marine accidents have greatly affected the shipping and marine production. The methods to improve the efficiency of marine search and rescue have gained popularity among researchers [1–3]. Due to the particularity of sea conditions, the drifting characteristic of the objects is a key factor for rapid search and rescue [4, 5].

Nowadays, massive efforts have been down in predicting the trajectory, including human motion [6, 7], intelligent vehicles [8–11], service robots [12], surveillance systems [13, 14], wind power generation [15, 16], magnetic field intensity [17, 18], and ship trajectory [19, 20]. The long short-term memory (LSTM) is a neural network that is responsible for calculating the dependence between observations in a time series. Therefore, it is often used for forecasting purposes. By using the temporal dependence-based LSTM networks, Liu et al. predicted the ocean-temperature changes successfully [21]. Cruz and Bernardino used the LSTM associated with a pretrained convolutional neural network to improve the detection performance in videos captured by small aircraft [22]. Choi et al. used the LSTM to predict the occurrences of abnormally high water temperature phenomena [23]. Tang et al. proposed an improved LSTM model with a random deactivation layer to deal with the time series problem [24]. Zhao and Shi presented a method that consists of a density-based spatial clustering of applications with noise algorithm and the LSTM to cluster and predict the ship trajectory [25]. Park et al. proposed a marine intelligent collision avoidance algorithm, and the ship trajectory prediction model was developed by using bidirectional LSTM [26]. Gao et al. proposed a multistep prediction method for ship trajectory, by using a novel MP-LSTM method. The proposed method can be used to solve the problems of complex mapping relationships and large data requirements [27]. Although the LSTM can solve

the gradient disappearance and explosion problems of traditional recurrent neural networks, its accuracy still needs to be further improved for more accurate trajectory prediction schemes.

The dense neural network (DNN) is one of the most classic neural networks. It has the merits of easy to understand and convenient to apply [28]. Moreover, it shows excellent fitting ability for most nonlinear functions. Once the depth of the fully connected neural network is increased, the function can be accurately fitted. The algorithm that combines the LSTM and the DNN can further improve the accuracy and flexibility of predicting trajectories. However, the application of LSTM algorithm in the marine mainly focuses on ship trajectory prediction. Researches on the marine drifting trajectory prediction model focus on smaller and unmotivated target are rarely reported so far, especially those based on the LSTM-DNN algorithm.

In this paper, we are interested in the prediction of the marine drifting trajectory, which can be used in the marine rapid search and rescue. The remote sensing of marine drifting trajectory prediction model is build based on the LSTM-DNN algorithm. Meanwhile, the information such as wind field, temperature field, ocean current motion field, and target attributes are included, and the influences of the above information on the trajectory model are studied in detail. The marine experiments are carried out to verify the accuracy of the proposed model. The conventional LSTM-based prediction model is used for comparison. By introducing DNN into the LSTM algorithm, the accuracy of drifting trajectory can be significantly improved. A detailed comparison of the two algorithms has also been given in this paper. The proposed remote sensing of marine drifting trajectory model can provide a high accurate trajectory prediction and will lead an important guidance in the marine search and rescue work. This work is aimed at investigating a high accurate and rapid prediction model for marine drifting trajectory. The contribution of the paper is as follows:

(1) The DNN is introduced into the conventional LSTM-based prediction model. A detailed comparison between the LSTM and LSTM-DNN-based model has been studied

(2) Compared with the conventional LSTM-based marine drifting trajectory model, the proposed model shows the merits of high accuracy

(3) The marine drifting trajectory database under the condition of ocean current and drifting, environmental field, target physical properties, and prediction duration is established by trials

The rest chapters of this paper are arranged as follows. Some related works are discussed in Section 2. The principle of the LSTM-DNN-based model is presented. System model and problem formulation are presented in Section 3. In Section 4, the test scheme is presented, and the real data and the simulation results are given to verify the correctness and the accuracy of the proposed model. And the conclusion part is shown in Section 5.

2. Related Work

In literature, several research works are related to the marine trajectory prediction, including the ship trajectory prediction mentioned in the introduction part. In addition to predicting the trajectory of marine ships, some researches have also been down on the trajectory prediction for marine search and rescue. For example, Zhu et al. proposed an ensemble trajectory prediction model for maritime search and rescue [29]. The authors proposed a regional subgrid velocity model based on drifting buoy data, and the proposed model is used to simulate the unsolved velocity that composed of turbulence and advection simulation errors. In Ref. [30], a drifting trajectory prediction model based on the object shape and stochastic motion features was proposed. Compared to the traditional factors of wind and currents, the proposed method also involved the effects of the object shape and stochastic motion features. Meanwhile, the computer simulation-based method was used to estimate the uncertainty parameters of the stochastic factors of the drifting objects. By using the model for the trajectories of objects drifting at the ocean surface, Blanken et al. proposed a fuzzy number-based framework for quantifying and propagating uncertainties [31]. Based on historical HF coastal radar data sets, Jitkajornwanich et al. proposed a predictive model for future current data [32]. By utilizing association rule mining combined with an object dispersion concept, the full potential of HF radar systems was exploited. Shchekinova et al. used the high-resolution ocean forecast and atmospheric data to solve the effects caused by the wind-induced drift on Lagrangian trajectories of surface sea objects [33].

In this paper, we focus on designing a marine drifting trajectory prediction model that can be used in the field of marine search and rescue. Based on the LSTM-DNN algorithm, a highly accurate prediction model of marine drifting trajectory is proposed.

3. System Model

An independent satellite maritime rescue system is established based on LSTM-DNN algorithm, satellite communication, and marine environment information The LSTM-DNN algorithm is used to deduce the real-time dynamic information of the overboard target needing to be searched and rescued.

3.1. The LSTM-DNN Predicting Model. Figure 1 shows the schematic diagram of the remote sensing of the marine drifting trajectory model. The proposed model is mainly composed of LSTM, DNN, and embedded encoder. The environment field information is processed by embedded encoder. The marine environment field variables are encoded into drifting data features by embedded encoder. In this paper, the marine environmental information includes current trajectory motion field, wind field, and temperature field. Each embedded encoder encodes an environmental information, in which the input of current trajectory motion field is the longitude and latitude coordinates and velocity component of the time and position corresponding

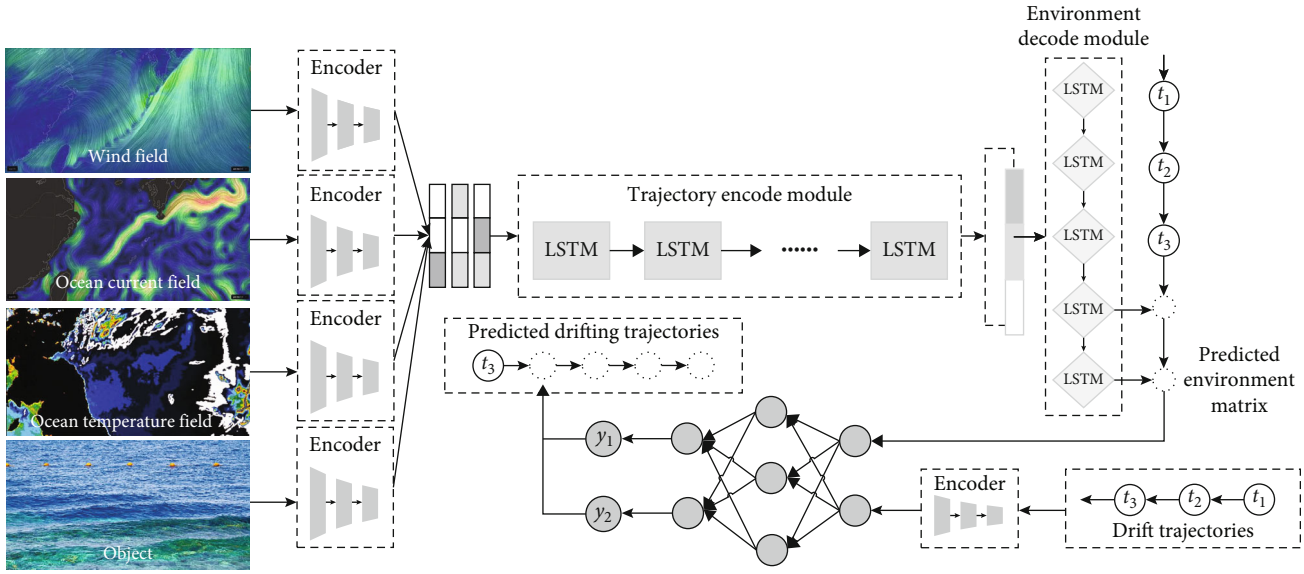

Figure 1: The schematic diagram of the remote sensing of the marine drifting trajectory model.

to the drift, and the velocity component is the east component and the north component, respectively. The input of wind field is the velocity component at the coordinate corresponding to the drift. The input of the temperature field is the ocean surface temperature of the drifting path. The encoding process is to calculate the characteristic matrix of the corresponding drifting track in the same time period according to the initial state of each marine environment variable and the longitude and latitude coordinates of each component and take the matrix and the characteristic matrix of drifting track data as the input of the drifting track prediction submodule. The environmental characteristic matrix of the future time is predicted in the trajectory encode module, and the obtained matrix is fused with the drift trajectories into the DNN module to predict the drifting track coordinates at the future time. Trajectory encode module is mainly responsible for fusing environmental data matrix. Environment decode module is mainly responsible for predicting future environmental information.

N_1, N_2, N_3, and N_4 represent the ocean current tracks, wind field data, temperature field, and N_4 drifting track, respectively. There is $N = N_1 + N_2 + N_3 + N_4$. The ocean current track data can be represented by $O_1, O_2, \cdots, O_{N_1}$, the wind field corresponding to each ocean current can be represented by $W_1, W_2, \cdots, W_{N_2}$, the drifting track data is represented by $P_1, P_2, \cdots, P_{N_4}$, and the temperature is represented by $K_1, K_2, \cdots, K_{N_3}$. Normalize the data of the same time node, and the data coordinates of the i th track at the time node be expressed as $S_i^t = (x_i^t, y_i^t)$, where $o_1, o_2, \cdots, o_{N_1}$, $p_1, p_2, \cdots, p_{N_1} \in i$, input the coordinate point of the above trajectory at $t = 1, 2, \cdots, t_o$ time. Based on the environmental prediction submodule, output the trajectory characteristic data x_i of marine environmental variables at $t = t_{0+1}$, $t_{0+2}, \cdots, t_{pred}$ time; then, the matrix x_i and drifting trajectory data p_i are used as the inputs of the drifting trajectory prediction submodule to further learn the time correlation between environmental variables at different locations and drifting trajectory variables through the DNN layer. Through the module, the drifting track coordinates at $t = t_{0+1}, t_{0+2}, \cdots, t_{pred}$ can be calculated. The environment prediction submodule is composed of a stacked LSTM network.

3.2. Equations. All figures and tables should be cited in the main text as Figure 1, Table 1, etc. In the proposed marine drifting trajectory model, the ocean current trajectory data, wind field, and temperature field are encoded into the input characteristic matrix of the environmental prediction submodule by the embedded encoder, represented by $x_i = \{\overrightarrow{x_1}, \overrightarrow{x_2}, \cdots, \overrightarrow{x_N}\}$. The environment prediction submodule is mainly composed of input module, redundancy module, and output module; x_i^t is the characteristic matrix of marine environmental variables at time t; h_i^{t-1} is the short-term memory matrix output by LSTM at time $t-1$; s_i^{t-1} is the long-term memory matrixoutput by LSTM at time $t-1$; then, the input module can be expressed as

$$a_\xi^t = \sum_{i=1}^{I} W_{i\xi} x_i^t + \sum_{h=1}^{H} W_{h\xi} b_h^{t-1} + \sum_{c=1}^{C} W_{C\xi} S_c^{t-1}, \quad (1)$$

where $W_{i\xi}$ represents the weight coefficient matrix between the incoming environment data matrix x_i and the input module, $W_{h\xi}$ represents the weight coefficient matrix between the short-term memory unit and the input module at time $t-1$, $W_{c\xi}$ represents the weight coefficient matrix between the long-term memory unit and the input module at time $t-1$, b_h^{t-1} is the short-term memory unit matrix, S_C^{t-1} is the long-term memory unit matrix, $b_\xi^t = f(a_\xi^t)$ is obtained through the activation function, and the activation function is tanh, which makes a linear transformation and

Table 1: Evaluate results.

	Start time: 2021-12-15 11:27 end time: 2021-12-15 17:37					
	Positioning time	Latitude	Longitude	Speed	Direction	Positioning mode
1	2021/12/15 11:27	38.85251	121.6708	0	157	GPS
2	2021/12/15 11:37	38.85313	121.6709	7.41	331	GPS
3	2021/12/15 11:48	38.85375	121.6706	0	331	GPS
4	2021/12/15 11:57	38.85439	121.6707	3.7	119	GPS
5	2021/12/15 12:07	38.85513	121.671	14.82	10	GPS
6	2021/12/15 12:17	38.8562	121.6718	3.7	19	GPS
7	2021/12/15 12:27	38.85708	121.673	18.52	309	GPS
8	2021/12/15 12:47	38.85844	121.6758	1.85	345	GPS
9	2021/12/15 13:37	38.862	121.6876	7.41	161	GPS
10	2021/12/15 13:57	38.86253	121.6946	0	161	GPS

nonlinear mapping on the data to improve the convergence speed of the model.

The redundant module can be expressed as

$$a_{\varphi}^{t} = \sum_{i=1}^{I} W_{i\varphi} x_i^t + \sum_{h=1}^{H} W_{h\varphi} b_h^{t-1} + \sum_{c=1}^{C} W_{C\varphi} S_c^{t-1}, \tag{2}$$

where W_{φ} represents the weight coefficient matrix between the incoming environment data matrix x_i and the input module, the weight coefficient matrix between the short-term memory unit and the input module at time $t-1$, and the weight coefficient matrix between the long-term memory unit and the input module at time $t-1$. The $b_{\varphi}^{t} = f(a_{\varphi}^{t})$ is obtained through the activation function.

The final data matrix is calculated by the output module to obtain the updated environment data matrix, which can be expressed as

$$a_{\omega}^{t} = \sum_{i=1}^{I} W_{i\varphi} x_i^t + \sum_{h=1}^{H} W_{h\omega} b_h^{t-1} + \sum_{c=1}^{C} W_{c\omega} S_c^{t-1}. \tag{3}$$

Activate get $b_{\omega}^{t} = f(a_{\omega}^{t})$.

The state matrix of neurons can be expressed as

$$a_c^t = \sum_{i=1}^{I} W_{ic} x_i^t + \sum_{h=1}^{H} W_{hc} b_h^{t-1}, \tag{4}$$

$$S_c^t = b_{\varphi}^t S_c^{t-1} + b_{\xi}^t g\left(a_c^t\right). \tag{5}$$

The output matrix of the final environmental prediction submodule can be expressed as

$$q_i = b_{\omega}^t h\left(S_c^t\right). \tag{6}$$

The output q_{i} and drifting track data matrix p_{i} are transmitted to the drifting track path prediction submodule, and the matrix $q_{\mathrm{i}}, p_{\mathrm{i}}$ is output through DNN network, drifting track coordinates at $t = t_1, t_2, \cdots, t_{pred}$ in the future are output through linear network. The whole process is shown in Figure 2.

The characteristic state matrix of DNN intermediate hidden layer is calculated by the following formula.

$$z = w^{(1)} * \left(\vec{\alpha}\right)^T + \left(b^{(1)}\right)^T. \tag{7}$$

In the formula, $\vec{\alpha} = [q_{\mathrm{i}}, p_{\mathrm{i}}]$, the weight coefficient matrix is expressed as

$$w^{(1)} = \begin{bmatrix} w(q_i, 1), w(p_i, 1) \\ w(q_i, 2), w(p_i, 2) \\ w(q_i, 3), w(p_i, 3) \end{bmatrix}, b^{(1)} = [b_1, b_2, b_3]. \tag{8}$$

Finally, the predicted value is

$$\hat{y} = w^{(2)} z^T + \left(b^{(2)}\right)^T. \tag{9}$$

In the formula, the weight coefficient matrix is expressed as

$$w^{(2)} = \begin{bmatrix} w(1,4), w(2,4), w(3,4) \\ w(1,5), w(2,5), w(3,5) \end{bmatrix}, b^{(2)} = [b_4, b_5]. \tag{10}$$

4. Test Scheme

In this paper, the real data from the northern sea area of the Yellow Sea in Dalian is used to train the proposed network framework. Among them, the ocean current trajectory data, wind field, and temperature field are obtained by field measurement, and the drifting trajectory data is obtained by simulating the real drifting test of counterweight buoy in the sea. Through the visual analysis of the data, the displacement generated by the current track and drifting track changes little in a short time, which can be regarded as uniform linear motion.

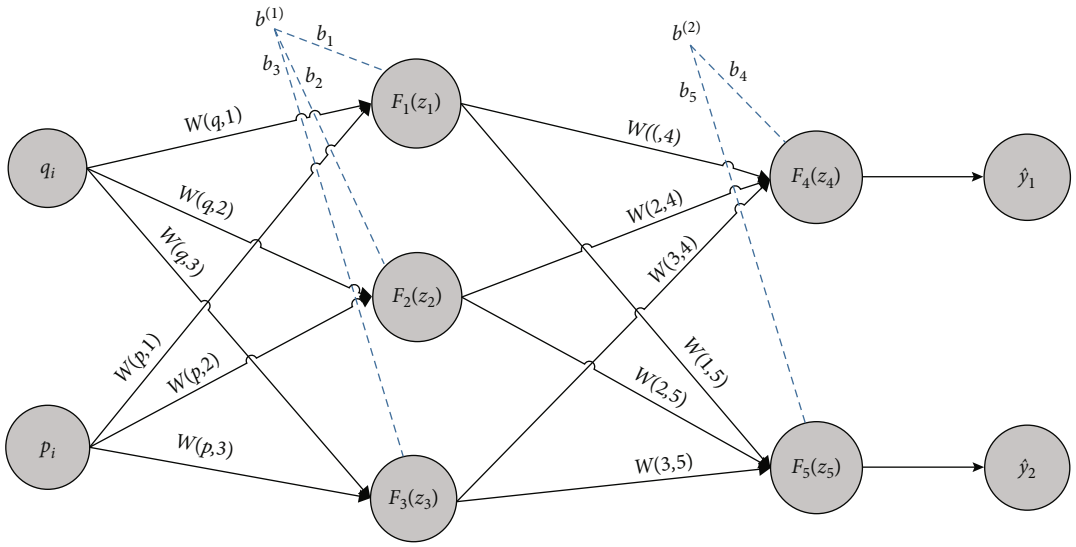

Figure 2: The output architecture of the DNN linear network.

Figure 3: Unequal volume circular scale.

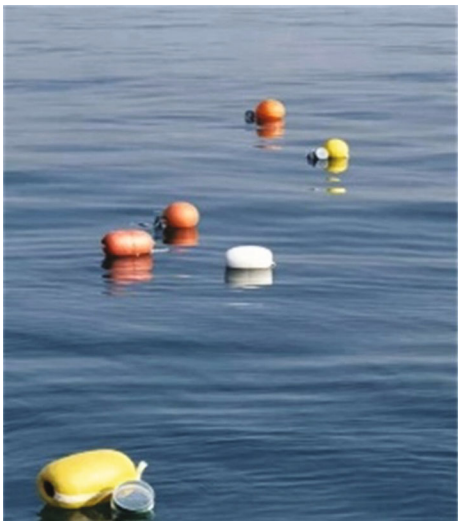

Figure 4: Drifting buoy.

4.1. Data Acquisition Scheme. In the same sea area located in the north of the Yellow Sea in Dalian, the water temperature from the ocean surface to 30 m below the sea is tested based on sensor conductivity temperature depth (CTD) equipment.

As shown in Figure 3, buoys with GPS positioning information are configured, including 40 buoys with different volumes with a diameter of about 6-30 cm. The forty buoys (different volumes) are thrown at a distance of 2 km offshore Dalian. After the current exchange period, the longitude and latitude information and direction data of buoys in different periods are recorded, respectively, and each buoy is divided into a group of drifting data.

Anemometer is used to record the wind speed; direction and the atmospheric temperature data at the place where the buoy is released. The ocean current data can be obtained by releasing drifting bottles every 500 m within 2 kilometers, so that there will be five drifting bottles used to record ocean current data. And then record the longitude, latitude, and direction data three hours after the current exchange period as the ocean current reference data.

Table 2: Wind field data.

	Wind speed (m/s)	Direction (°)
Point 1	0	358
Point 2	2.4	354
Point 3	2.2	355
Point 4	0	358
Point 5	2.9	356

4.2. Test Process. Training data collection:

Prepare the experimental ship and carry the GPS sealed bottle, CTD, buoy, anemometer, and other equipment.

Drive the ship to the northern sea area of the Yellow Sea, and release a sealed bottle and a group of buoys every 0.5 km

Table 3: Temperature field data.

Data	Vbatt [V]	Press [dBar]	Temp [°C]	Sound [m/s]	Sigma [kg/m^3]	Time	Date
1	6.27	0.16	9.43	1445.02	-0.25	11 : 20 : 55	2021/12/15
2	6.26	0.17	9.44	1445.03	-0.25	11 : 20 : 55	2021/12/15
3	6.26	0.16	9.44	1445.07	-0.25	11 : 20 : 55	2021/12/15
4	6.26	0.16	9.45	1445.1	-0.25	11 : 20 : 55	2021/12/15
5	6.26	0.14	9.46	1445.12	-0.25	11 : 20 : 55	2021/12/15
6	6.26	0.16	9.46	1445.15	-0.25	11 : 20 : 56	2021/12/15
7	6.27	0.16	9.47	1445.17	-0.25	11 : 20 : 56	2021/12/15
8	6.26	0.17	9.48	1445.19	-0.25	11 : 20 : 56	2021/12/15
9	6.27	0.14	9.48	1445.21	-0.25	11 : 20 : 56	2021/12/15
10	6.26	0.16	9.48	1445.22	-0.25	11 : 20 : 56	2021/12/15

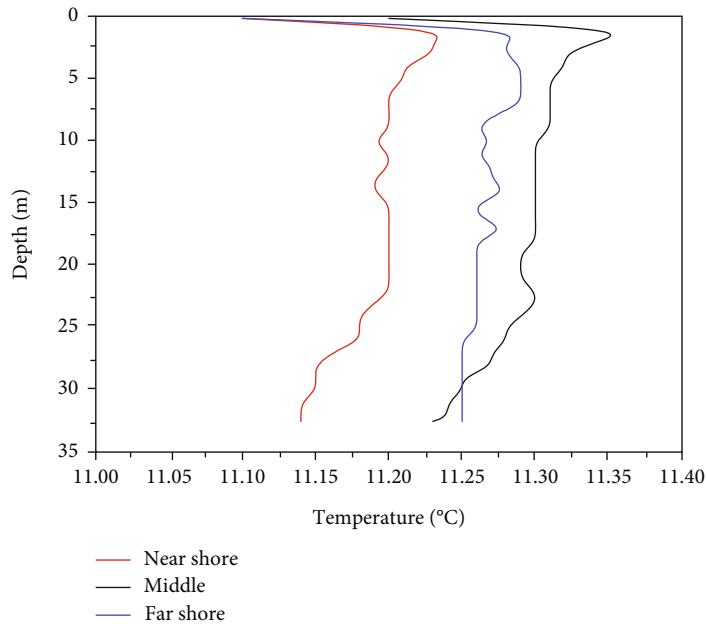

Figure 5: Temperature change curve of near shore release point, middle release point, and far shore release point during descent.

(eight buoys in a group, different specifications, and pre-prepared groups), a total of five groups as shown in Figure 4.

After the release, the information of sea surface wind field and temperature field is measured and the data is recorded.

Record the drifting position information of the separate sealed bottle for three hours, which can be used as ocean current data. Record the three-hour buoy position information, which is the drifting track. During this time, the data can be preprocessed according to the model requirements.

After waiting for three hours, count the overall data, import the data into the model for training after data preprocessing, and save the model.

Prediction stage:

Drive the ship to 2 km off the coast of Dalian.

Release buoy and life jacket with GPS positioning signal.

Record the position information of coordinate points every 10 minutes when the buoy floats.

After data preprocessing, the first four floating positions and the positions sent by personnel are transferred to the pretrained model to obtain the predicted position information of the next time node, record the corresponding data, and drive the ship to search for drift near the coordinate point.

4.3. Data Processing. Based on the above test process, the following ocean current trajectory data are collected, some of which are shown in Table 1.

The longitude and latitude coordinates, motion speed, and motion direction of the current track are collected in Table 1 every ten minutes. The lack of time data means that the original coordinates of the object at this time node have not changed. During data processing, the longitude and latitude of adjacent nodes are used for filling. Similarly, the

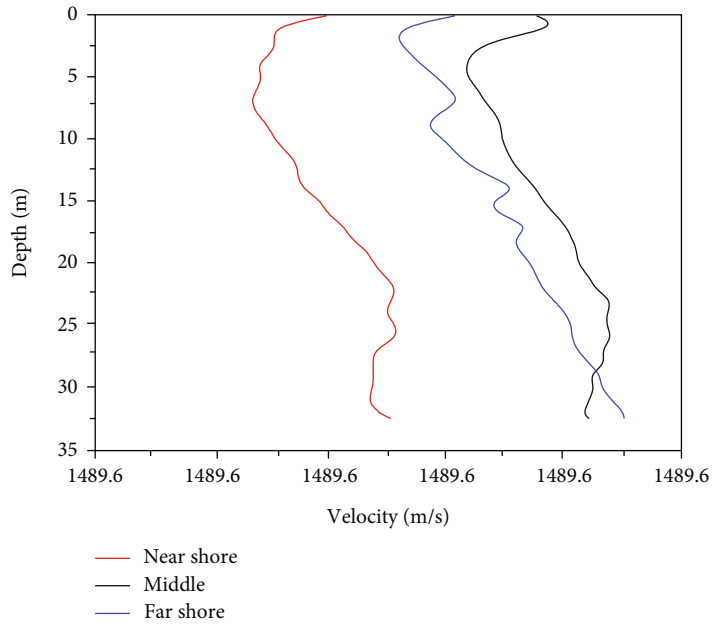

Figure 6: Sound velocity variation curve at near shore release point, middle release point, and far shore release point during descent.

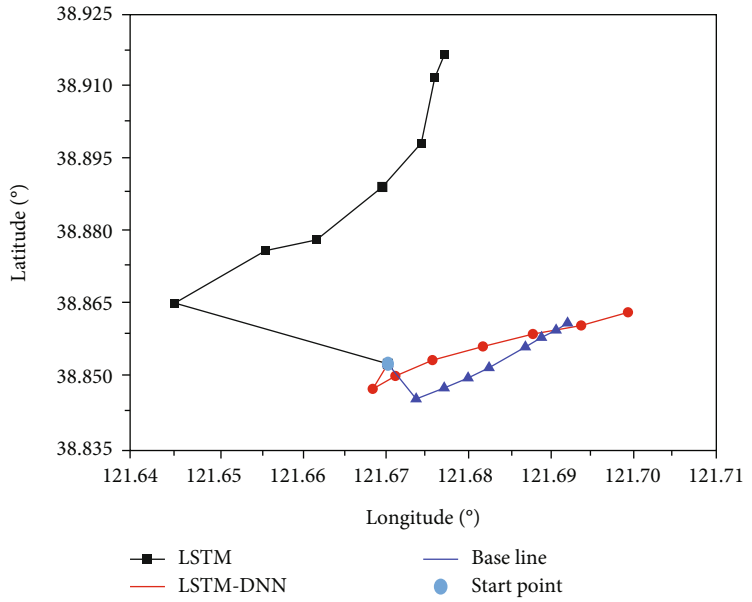

Figure 7: Comparison diagram of observed trajectory and predicted future trajectory based on LSTM and LSTM-DNN.

drifting track motion data of the same dimension are collected and preprocessed accordingly.

The wind field information and temperature field information of each release point are collected according to the drifting track, and the environmental field data are recorded every ten minutes. Some data are shown in Tables 2 and 3.

In Table 3, the main parameters Vbatt represent voltage, press represents depth, temp represents temperature, sound represents sound velocity, and sigma represents salinity. During the temperature field acquisition, the equipment detected the depth data from the sea surface to 32 meters below the sea water and detected the environmental information of the five release points. Because the temperature field in the near sea area changes very little, it mainly analyzes the data information of the three positions, namely, the near coast release point, the middle release point, and the far coast release point. It mainly analyzes the change of temperature with depth and the change of sound velocity with depth during the decline process, as shown in Figures 5 and 6, respectively.

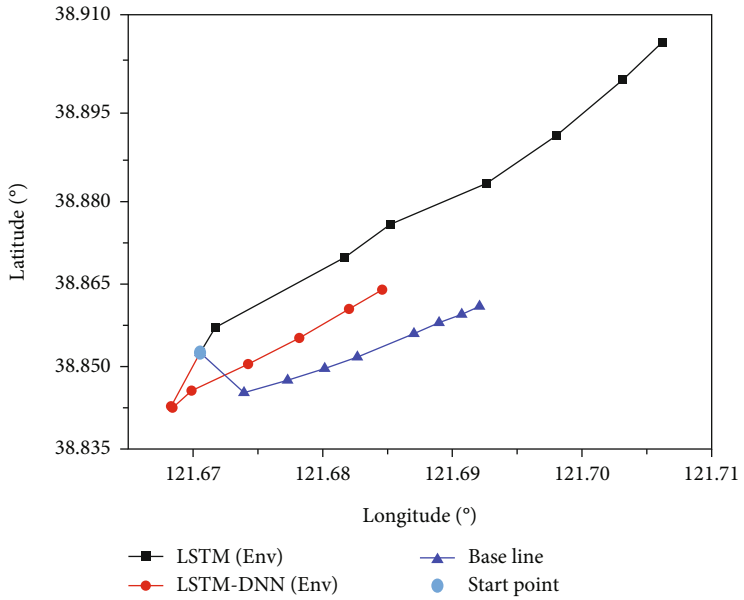

Figure 8: Comparison diagram of observed trajectory and predicted future trajectory based on LSTM and LSTM-DNN under the same environmental field.

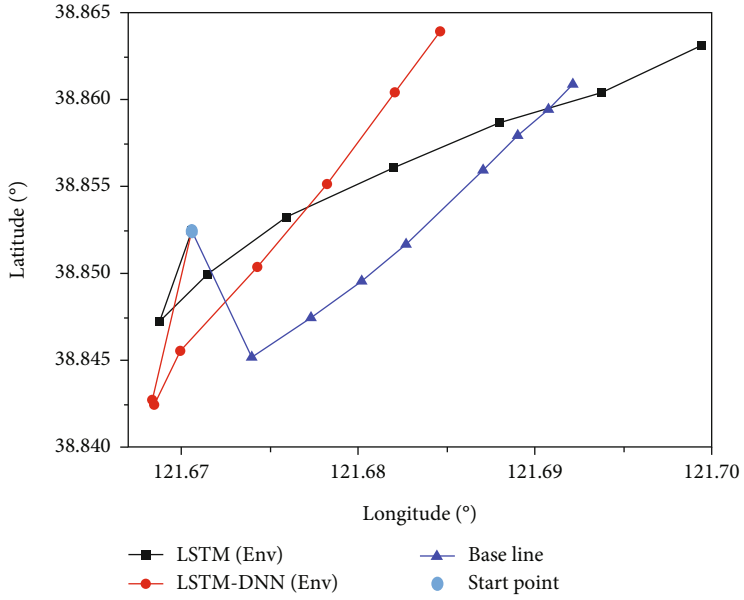

Figure 9: Comparison of LSTM-DNN observed orbits and predicted future orbits under the same environmental field.

According to the data processing and analysis, it can be determined that the temperature is approximately isothermal layer with depth, and the sound velocity is approximately weak positive gradient with depth. Therefore, in the preprocessing of temperature data, the temperature field can be approximately the mean value in the depth direction of the point, and the change of sound velocity can be ignored.

Collect the test data, mainly including the time stamp, latitude, longitude, speed, direction, target attribute, temperature field, wind field, and other parameters of each track, and save them in the LSTM-DNN model.

4.4. Performance of LSTM-DNN Predicting Model

(1) Influence of ocean current motion field on drifting trajectory

In order to explore the influence of ocean current trajectory on drifting trajectory, only ocean current data is added

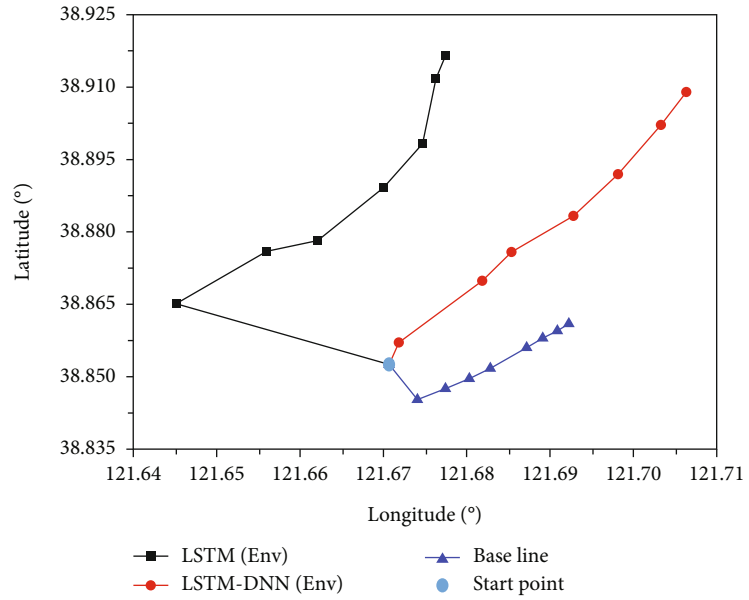

Figure 10: Comparison between LSTM observation orbit and predicted future orbit under the same environmental field.

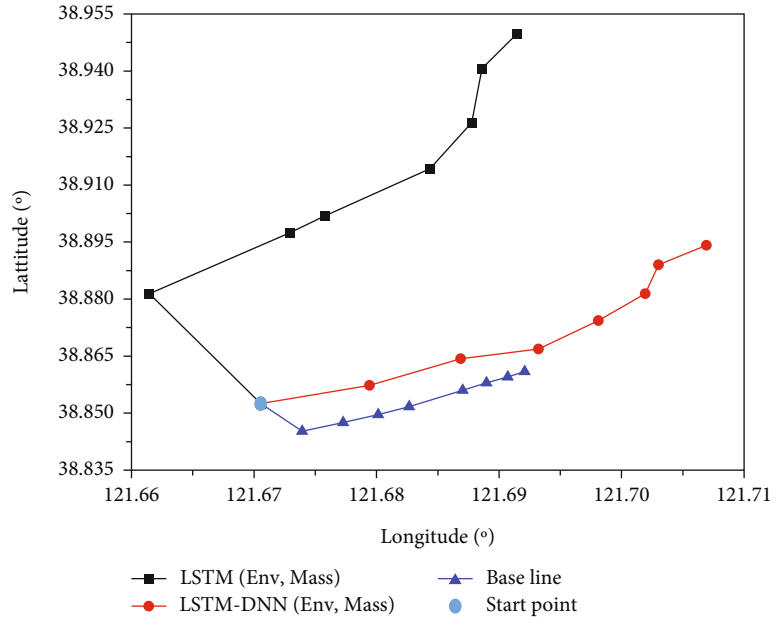

Figure 11: Comparison diagram of observed trajectory and predicted future trajectory based on LSTM and LSTM-DNN under the same target attributes.

during training analysis. The traditional LSTM model and LSTM-DNN model mentioned in this paper are trained, respectively, to model and predict the test data. The test results are shown in Figure 7.

The dot in Figure 7 is the initial position of the drifting track, the red track represents the predicted track based on the LSTM-DNN model, the black path represents the predicted track of the traditional LSTM model, and the blue track is the real acquisition path. It can be seen that under the same environment, the prediction result of LSTM-DNN is significantly better than that of LSTM model, in which the root mean squared error (RMSE) calculation result of LSTM-DNN model is 0.0332, and the RMSE result of LSTM is 0.0357. Therefore, LSTM-DNN has higher prediction accuracy.

(2) Analysis on the influence of wind field and temperature field on drifting trajectory

In order to explore the influence of wind field and temperature field on drifting trajectory, the preprocessed ocean current trajectory data in (1) is applied, the environmental

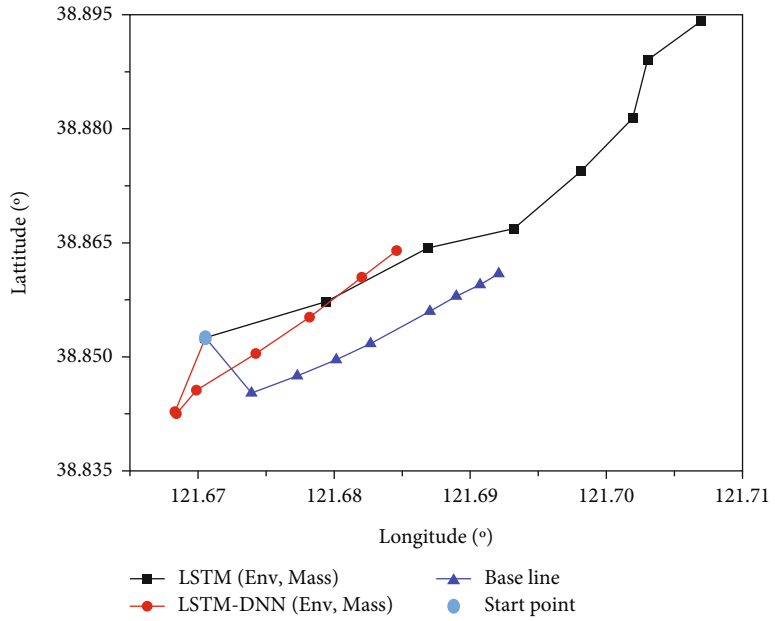

Figure 12: Comparison between LSTM-DNN observation orbit and predicted future orbit under the same target attributes.

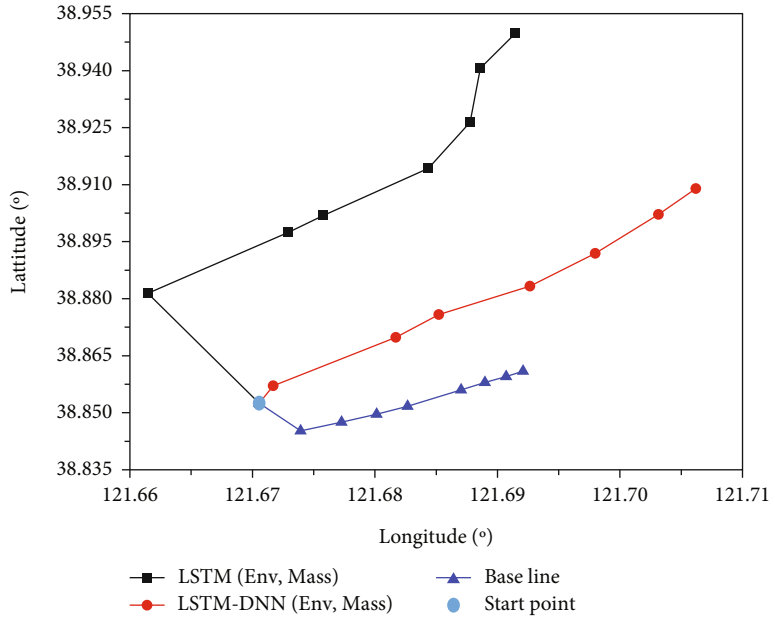

Figure 13: Comparison between LSTM observation orbit and predicted future orbit under the same target attributes.

field data is newly loaded into the training data, the LSTM model and LSTM-DNN model are further trained to predict the same set of test data, and the prediction results of the two models and the results of each model and (1) are analyzed and compared, respectively, as shown in Figure 8.

The dot in Figure 8 is the initial position of the drifting track, the red track represents the predicted track after adding the environmental field to the training data based on the LSTM-DNN model, the black path represents the predicted track after adding the environmental field to the training data of the traditional LSTM model, and the blue track is the real acquisition path. It can be seen that under the same environment, the prediction result of LSTM-DNN model is significantly better than that of the LSTM model. The RMSE calculation result of LSTM-DNN model is 0.0256, and the RMSE result of LSTM model is 0.0339. LSTM-DNN model has higher prediction accuracy.

Figures 9 and 10 show the analysis and comparison between the LSTM-DNN model, the LSTM model, and the original data after adding the wind field and temperature field environment, respectively. It can be seen that the prediction accuracy of both models is improved. Therefore,

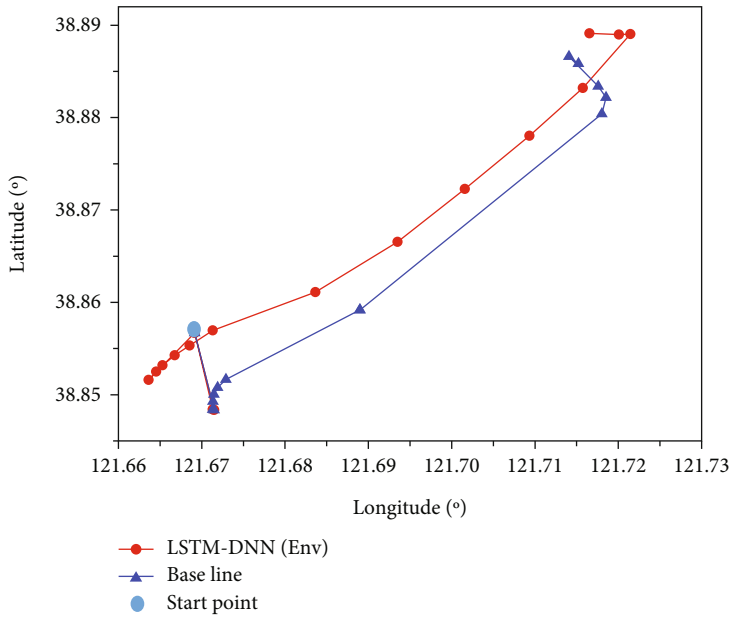

Figure 14: Comparison between observed orbit and predicted future orbit under 6 hours of LSTM-DNN model.

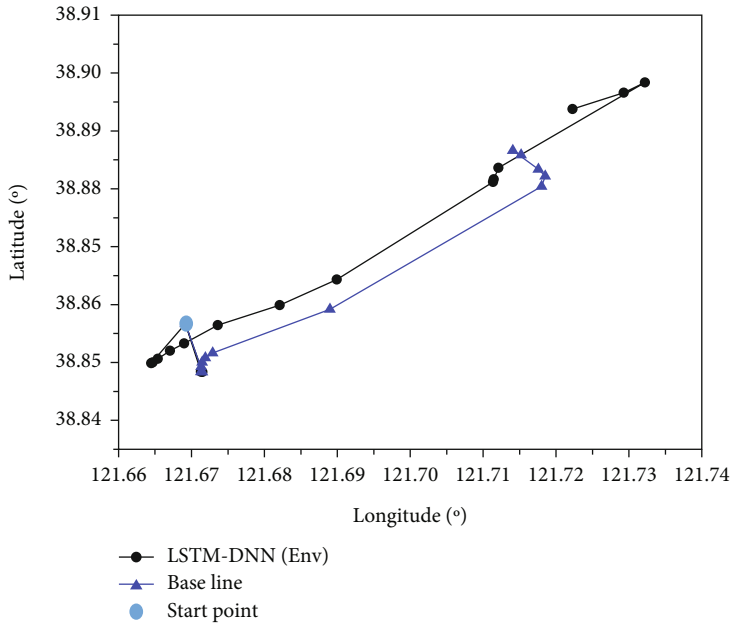

Figure 15: Comparison between observed orbit and predicted future orbit under 6 hours of LSTM model.

determining the prediction results of wind field and temperature field on drifting trajectory can improve its accuracy.

(3) Influence of target attributes on drifting trajectory

Under the same data, explore the impact of target object attributes on drifting trajectory, and set target attributes for each group of drifting objects, mainly shape, volume, and weight. The shape is converted into data format by one hot coding, and LSTM model and LSTM-DNN model are trained. The analysis and comparison prediction results are shown in Figure 11.

The dot marked as the start point in Figure 11 is the initial position of the drifting track. The red track represents the predicted track after adding the environmental field and target attribute in the training data based on the LSTM-DNN model. The black path represents the predicted track after adding the environmental field and target attribute in the training data of the traditional LSTM model, and the blue track is the real acquisition path. Under the same data, the RMSE calculation result of LSTM-DNN model is 0.0325. The RMSE result of LSTM model is 0.0343, and the prediction accuracy of the two models is lower than that of the environmental field. Therefore, the

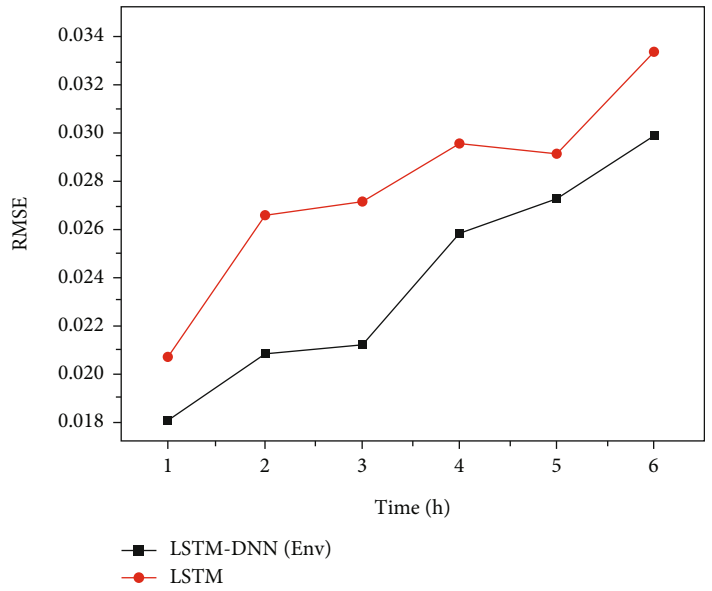

Figure 16: Comparison between LSTM-DNN and LSTM 6-hour prediction RMSE.

accuracy of the target's own attributes for drifting trajectory prediction will show a weak downward trend.

Figures 12 and 13 show the prediction results of the two models after adding the target attribute. By comparing the prediction accuracy, the accuracy of the prediction trajectory shows a weak downward trend after adding the target attribute on the basis of the environmental field. This is because the floating objects on the sea surface are mainly affected by environmental factors such as wind field and ocean current trajectory. Meanwhile, adding too many self attributes will increase the redundant characteristics of the model.

(4) Influence of prediction duration on prediction results of drifting trajectory

In this section, comparison between observed orbit and predicted future orbit under 6 hours base of the LSTM-DNN model and LSTM model is given. The tested data is in the same sea area, the first six groups of data are intercepted as the observation path trajectory, and the two models are used to predict the subsequent drift path. The results are shown in Figure 14 (LSTM-DNN model) and Figure 15 (LSTM model), respectively.

Figure 16 shows the comparison of LSTM-DNN model and LSTM model with the real path in 6 hours. The RMSE corresponding to 1st hour to 6th hour is calculated according to the predicted path, as shown in Figure 16. It can be observed that the prediction results of LSTM-DNN model in 6 hours are more accurate than LSTM model.

5. Conclusions

The marine drifting trajectory prediction method proposed in this paper modeled the environmental field based on LSTM-DNN. It can be used to predict the environmental information matrix at a point in the future and further transfer the environmental information matrix and the path information of the drifting trajectory into the DNN network; then, the drifting trajectory at a certain time in the future can be predicted. In this paper, the influence of ocean current motion field, environmental fields, and target attributes on the drifting trajectory is discussed in detail. Numerical results show that ocean current motion field and environmental fields have a relatively more obvious impact on the predicted results. The proposed model can provide a very accurate trajectory prediction in up to 6 hours. The proposed algorithm has a significant effect on short-term maritime trajectory prediction and will lead an important guide in the marine search and rescue work.

Data Availability

The data used to support the findings of this study are available from the corresponding author upon request.

Conflicts of Interest

The authors declare no conflict of interest.

Authors' Contributions

Conceptualization was done by Xianbin Li and Kai Wang; software was done by Xianbin Li and Kai Wang; writing—original draft preparation was done by Xianbin Li, Kai Wang, Min Tang, Jiangyi Qin, and Peng Wu; writing—review and editing was done by Min Tang, Kai Wang, Tingting Yang, and Haichao Zhang. All authors have read and agreed to the published version of the manuscript.

References

[1] E. Akyuz, "A marine accident analysing model to evaluate potential operational causes in cargo ships," *Safety Science*, vol. 92, pp. 17–25, 2017.

[2] J. Kwesi-Buor, D. A. Menachof, and R. Talas, "Scenario analysis and disaster preparedness for port and maritime logistics risk management," *Accident; Analysis and Prevention*, vol. 123, pp. 433–447, 2019.

[3] A. Ee, B. Ap, and A. Mv, "Statistical analysis of ship accidents and review of safety level," *Safety Science*, vol. 85, pp. 282–292, 2016.

[4] A. M. Zhang and H. G. Sui, "An intelligent marine search and rescue directing system," *Proceedings of SPIE - The International Society for Optical Engineering*, vol. 6421, 2006.

[5] Y. Yang, Y. Mao, R. Xie, Y. Hu, and Y. Nan, "A novel optimal route planning algorithm for searching on the sea," *Aeronautical Journal*, vol. 125, no. 1288, pp. 1064–1082, 2021.

[6] A. Rudenko, L. Palmieri, M. Herman, K. M. Kitani, D. M. Gavrila, and K. O. Arras, "Human motion trajectory prediction: a survey," *International Journal of Robotics Research*, vol. 39, no. 8, pp. 895–935, 2020.

[7] P. Lv, H. Wei, T. Gu et al., "Trajectory distributions: a new description of movement for trajectory prediction," *Computational visual media*, vol. 8, no. 2, pp. 213–224, 2022.

[8] J. Yan, Z. Peng, H. Yin et al., "Trajectory prediction for intelligent vehicles using spatial-attention mechanism," *IET Intelligent Transport Systems*, vol. 14, no. 13, pp. 1855–1863, 2020.

[9] F. Large, D. Vasquez, T. Fraichard, and C. Laugier, "Avoiding cars and pedestrians using velocity obstacles and motion prediction," *IEEE Intelligent Vehicles Symposium, IEEE*, pp. 375–379, 2004.

[10] L. Liu, M. Zhao, M. Yu, M. A. Jan, D. Lan, and A. Taherkordi, "Mobility-aware multi-hop task offloading for autonomous driving in vehicular edge computing and networks," *IEEE Transactions on Intelligent Transportation Systems*, pp. 1–14, 2022.

[11] J. Feng, L. Liu, Q. Pei, and K. Li, "Min-max cost optimization for efficient hierarchical federated learning in wireless edge networks," *IEEE Transactions on Parallel and Distributed Systems*, p. 1, 2022.

[12] S. Thompson, T. Horiuchi, and S. Kagami, "A probabilistic model of human motion and navigation intent for mobile robot path planning," in *2009 4th International Conference on Autonomous Robots and Agents*, pp. 663–668, IEEE, 2009.

[13] M. Luber, J. A. Stork, G. D. Tipaldi, and K. O. Arras, "People tracking with human motion predictions from social forces," in *2010 IEEE International Conference on Robotics and Automation*, pp. 464–469, IEEE, 2010.

[14] B. Musleh, F. García, J. Otamendi, J. M. Armingol, and A. De la Escalera, "Identifying and tracking pedestrians based on sensor fusion and motion stability predictions," *Sensors*, vol. 10, no. 9, pp. 8028–8053, 2010.

[15] E. Mohammed, S. Wang, and J. Yu, "Ultra-short-term wind power prediction using a hybrid model," *Science*, vol. 63, p. 012005, 2017.

[16] Q. Wu, F. Guan, C. Lv, and Y. Huang, "Ultra-short-term multi-step wind power forecasting based on CNN-LSTM," *IET Renewable Power Generation*, vol. 15, no. 5, pp. 1019–1029, 2021.

[17] J. Wu, X. Yang, H. Wang, J. Chen, Q. Zhao, and B. Xiao, *Study on Prediction Model of Magnetic Field Intensity of Submarine Power Cable Based on LSTM*, Pervasive Health: Pervasive Computing Technologies for Healthcare, 2020.

[18] S. N. Khotimah and S. Viridi, "Influence of initial velocity on trajectories of a charged particle in uniform crossed electric and magnetic fields," *European Journal of Physics*, vol. 38, no. 2, p. 025204, 2017.

[19] W. Luo and G. Zhang, "Ship motion trajectory and prediction based on vector analysis," *Journal of Coastal Research*, vol. 95, no. sp1, pp. 1183–1188, 2020.

[20] C. Tang, M. Chen, J. Zhao et al., "A novel ship trajectory clustering method for finding overall and local features of ship trajectories," *Ocean Engineering*, vol. 241, p. 110108, 2021.

[21] J. Liu, T. Zhang, G. Han, and Y. Gou, "TD-LSTM: temporal dependence-based LSTM networks for marine temperature prediction," *Sensors*, vol. 18, no. 11, p. 3797, 2018.

[22] G. Cruz and A. Bernardino, "Learning temporal features for detection on maritime airborne video sequences using convolutional LSTM," *IEEE Transactions on Geoscience and Remote Sensing*, vol. 57, no. 9, pp. 6565–6576, 2019.

[23] H. M. Choi, M. K. Kim, and H. Yang, "Abnormally high water temperature prediction using LSTM deep learning model," *Journal of Intelligent Fuzzy Systems*, vol. 40, no. 4, pp. 8013–8020, 2021.

[24] G. Tang, J. Lei, C. Shao, X. Hu, W. Cao, and S. Men, "Short-term prediction in vessel heave motion based on improved LSTM model," *IEEE Access*, vol. 9, pp. 58067–58078, 2021.

[25] L. Zhao and G. Shi, "Maritime anomaly detection using density-based clustering and recurrent neural network," *Journal of Navigation*, vol. 72, no. 4, pp. 894–916, 2019.

[26] J. Park, J. S. Jeong, and Y. S. Park, "Ship trajectory prediction based on bi-LSTM using spectral-clustered AIS data," *Journal of marine science and engineering*, vol. 9, no. 9, p. 1037, 2021.

[27] D. W. Gao, Y. S. Zhu, J. F. Zhang, Y. K. He, K. Yan, and B. R. Yan, "A novel MP-LSTM method for ship trajectory prediction based on AIS data," *Ocean Engineering*, vol. 228, p. 108956, 2021.

[28] Y. Heng, Y. Jian-Ping, and Xing, "Study on dam deformation prediction based on deep fully connected neural network [J]," *Geodesy and Geodynamics*, vol. 41, no. 2, pp. 162–166, 2021.

[29] K. Zhu, L. Mu, and X. Xia, "An ensemble trajectory prediction model for maritime search and rescue and oil spill based on sub-grid velocity model," *Ocean Engineering*, vol. 236, p. 109513, 2021.

[30] S. Z. Wang, H. B. Nie, and C. J. Shi, "A drifting trajectory prediction model based on object shape and stochastic motion features," *Journal of Hydrodynamics*, vol. 26, no. 6, pp. 951–959, 2014.

[31] H. Blanken, C. Valeo, C. G. Hannah, U. T. Khan, and T. Juhász, "A fuzzy-based framework for assessing uncertainty in drift prediction using observed currents and winds," *FMARS*, vol. 8, 2021.

[32] K. Jitkajornwanich, P. Vateekul, U. Gupta et al., "Ocean surface current prediction based on HF radar observations using trajectory-oriented association rule mining," in *2017 IEEE international conrerence on big data (big data)*, pp. 4293–4300, Boston, MA, 2017.

[33] E. Y. Shchekinova, Y. Kumkar, and G. Coppini, "Numerical reconstruction of trajectory of small-size surface drifter in the Mediterranean Sea," *Ocean Dynamics*, vol. 66, no. 2, pp. 153–161, 2016.